








# Photo-acoustic technique with widely tuneable laser: Metasurface circular dichroism response

Claudia Skubisz<sup>1</sup> , Emilija Petronijevic<sup>1,\*</sup> , Grigore Leahu<sup>1</sup>, Tiziana Cesca<sup>2</sup> , Carlo Scian<sup>2</sup> , Giovanni Mattei<sup>2</sup> , Concita Sibilia<sup>1</sup> , and Alessandro Belardini<sup>1</sup> 

<sup>1</sup>Department SBAI, Sapienza University of Rome, Via Antonio Scarpa 14-16, 00161 Rome, Italy

<sup>2</sup>Department of Physics and Astronomy, University of Padova, Via Marzolo 8, I-35131 Padova, Italy

Received 1 March 2024 / Accepted 3 April 2024

**Abstract.** Chirality, an intrinsic property of certain entities in the universe, is characterized by the absence of mirror symmetry. Understanding chirality is crucial as it influences molecular interactions and properties. Circular dichroism (CD), measured using circularly polarized light, is a standard technique for probing chirality, but its sensitivity is often limited. Here, we explore extrinsic chirality (i.e. a property arising from asymmetric achiral materials when observed from out of normal incidence directions), using photo-acoustic spectroscopy (PAS). PAS allows direct measurement of local absorption, by monitoring the heat produced and transferred to the surrounding air, regardless the transmitted, reflected, and scattered light that flows away from the sample. In conventional techniques, the CD is usually measured by taking into account only the extinction as transmitted (or reflected) light. In this study, we introduce a new PAS setup that employs an oblique-incidence laser to study extrinsic chirality in silver-coated self-assembled metasurfaces. Our experimental results reveal intriguing CD trends dependent on the angle of incidence and wavelength, indicative of extrinsic chirality. This study expands the application of PAS, enabling simultaneous analysis of multiple wavelengths and providing valuable insights into chiral metasurfaces.

**Keywords:** Nanostructures, Extrinsic chirality, Photo-acoustic spectroscopy, Circular dichroism.

## 1 Introduction

Chirality is a fundamental property of some components of our universe, characterized by the absence of specular symmetry in an object [1]. A chiral object and its mirror image are called enantiomers and although they have the same physical constituents, this lack of specular symmetry influences the interaction of the enantiomer with the external world. Chirality is a common property of many molecules [2]. Circularly polarized light is conventionally used to probe the chirality of the sample; left and right circular polarizations (LCP and RCP, respectively) are absorbed differently, and this difference is defined as Circular Dichroism (CD) [3]. However, since the natural CD of chiral molecules is extremely low, conventional CD techniques are bulky and have low sensitivity. Fortunately, nanostructures can be designed to boost CD signal of chiral molecules [4, 5]. To obtain CD, nanostructures do not need to be chiral themselves: instead, chirality can be induced by combining the asymmetry of the sample and the optical set-up. This property is called extrinsic chirality and it is obtained by

breaking the symmetry of the light-sample interaction by forming a non-planar triad of vectors between the light wave-vector, the normal of the sample's surface, and the vector of the sample's asymmetry [6, 7]. In reference [8], the chiral optical response was induced in 2-D mirror-symmetric nanostructures (trimers) by chosen heterogeneous material composition which breaks the symmetry of the system. In references [9, 10] similar geometries, but with magnetic materials allows the magnetic control of the induced CD. In our previous works, we measured extrinsic chirality with different conventional techniques such as extinction [11] and reflection [12]. However, to directly measure the absorption response, unconventional photo-thermal techniques can be applied [13–18].

Photo-acoustic spectroscopy (PAS) is a photothermal technique that exploits the interaction between an incident light beam and matter, inducing a non-radiative de-excitation process that generates heat [19]. When the light intensity is modulated over time, a sample confined in a sealed chamber filled with air undergoes alternating cycles of heating and cooling, resulting in air pressure variations. These fluctuations produce an acoustic signal, which is then converted into an electrical signal through a

\* Corresponding author: [emilija.petronijevic@uniroma1.it](mailto:emilija.petronijevic@uniroma1.it)

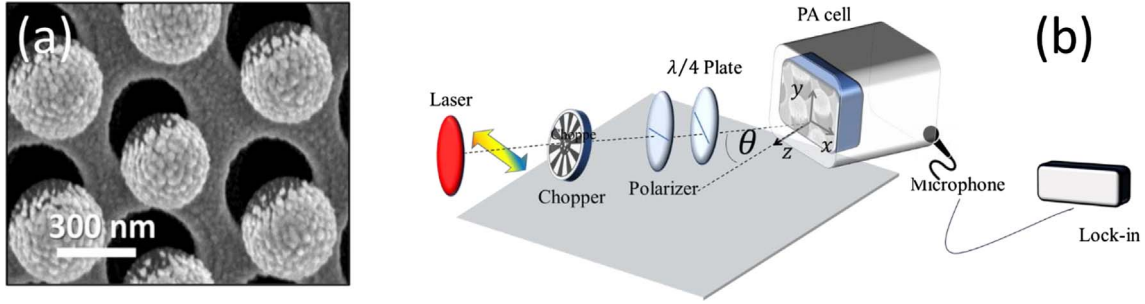


**Fig. 1.** (a) SEM image of the realized sample. (b) Schematic of the experimental set-up

sensitive microphone coupled with a lock-in amplifier. This approach enables direct measurement of local absorption, thereby detecting effects that might otherwise be obscured by other scattering-dependent techniques, such as the extinction measurements performed in transmission [8] or in reflection [19], where the far field signal can be related with the local absorption in a non trivial way, as described, for example, in reference [20]. To characterize CD, we previously used only single laser wavelengths to precisely define the incident polarization (LCP or RCP), and have high enough incident power with respect to usual lamp light.

In this study, we introduce a new PAS set-up, based on a widely tunable near-infrared laser excitation under oblique incidence. We use it to measure the absorption and the extrinsic chirality of low-cost self-assembled metasurfaces asymmetrically covered by silver. PAS applied at multiple wavelengths highlights the presence of extrinsic chirality, in good agreement with previous theoretical predictions.

## 2 Results and discussion

In [Figure 1a](#), the scanning electron microscopy (SEM) image of the investigated sample is shown. The experimental arrangement utilized for the measurements (see [Fig. 1b](#)) comprises a laser that covers a spectral range from 680 nm to 1000 nm. The light emitted by the source undergoes modulation via a mechanical chopper operating at a fixed frequency of 81 Hz. Prior to reaching the sample housed within the photo-acoustic cell, the light beam traverses a polarizer and a quarter-wave plate. This setup allows for controlled polarization of the incident light. The photo-acoustic cell, where the sample is placed, is equipped with a rotating stage enabling examination of the sample at various angles of incidence ( $\theta$ ) relative to the normal surface.

For our specific study, the incidence angles employed span in the range of  $\theta = \pm 30^\circ$ . The impinging light has a spot diameter of 1.2 mm and is polarized either with linear horizontal polarization (p-pol.) or RCP and LCP. The signal detected by the microphone preamplifier is fed into a lock-in amplifier, which analyzes the signal in correlation with the modulation frequency of the light source. To minimize the influence of scattered light on the microphone's signal reception from the sample, a narrow-diameter – labyrinthine tunnel is employed.

The primary component of the photo-acoustic cell is a movable quartz cylinder with two optically polished faces. By adjusting the position of this cylinder along the  $z$ -axis, the distance between the sample surface and the window can be optimized, thereby minimizing the cell volume to enhance signal detection. Simultaneously, transmitted light exits the cell through the quartz cylinder, contributing to noise reduction in the signal. The metasurface investigated consists of hexagonal unit cells with a pitch of 518 nm, containing polystyrene (PS) nanospheres measuring approximately 370 nm in diameter. The whole metasurface has a size of around  $5 \times 5$  mm and was fabricated by nanosphere lithography [12, 13] onto a 0.3 mm glass substrate, and coated with a 55 nm thick layer of metallic silver (Ag) through thermal evaporation at a tilt angle of  $45^\circ$  relative to the sample surface. Due to the non-close packing arrangement of the 2D array, the metallic layer deposition resulted in the creation of a metallic grid on the substrate surface. The sample orientation in the PAS cell is fixed to follow the rules of extrinsic chirality: the projection of the Ag evaporation onto the sample surface is perpendicular to the plane of incidence.

[Figure 2](#) illustrates the trends of the PAS signal for three different values of the angle  $\theta = 0^\circ$ ,  $\theta = +15^\circ$ , and  $\theta = -15^\circ$ . It can be observed how the absorption levels of the sample, at various angles of incidence, present linearly decreasing trends as the value of the wavelength increases. The absorption for a zero angle is very similar for different polarizations and slightly decreases with increasing wavelengths. The absorption levels for angles of  $+15^\circ$  and  $-15^\circ$  exhibit larger oscillations and present a pronounced difference between circular polarizations. Several significant findings emerge from the obtained results. Firstly, CD measurements conducted with respect to the angle of incidence reveal intriguing trends. [Figure 3](#) shows that for wavelengths longer than 800 nm, the CD gradually increases from 0% at normal incidence, to positive values for positive angles of incidence, and changing to negative values as the incidence angles become more negative. This phenomenon, indicative of a sign reversal, is a characteristic feature of extrinsic chirality. Moreover, an interesting observation is noted concerning wavelengths at 800 nm in [Figure 3](#), where all CD trends converge to a value of 0%, suggesting a unique behavior of the sample at this specific wavelength. For wavelengths shorter than 800 nm the process is reversed. Additionally, the sample demonstrates a remarkable rapid variation in CD across a broad range of angles. This dynamic response

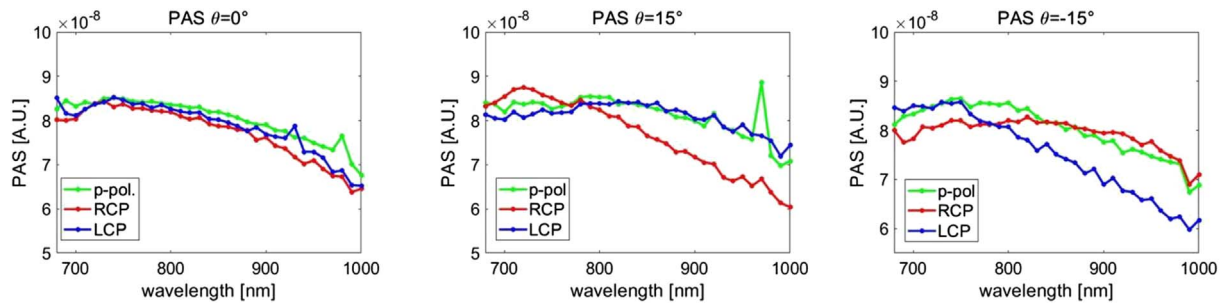


Fig. 2. Absorption level trends of the sample for various angles of incidence  $\theta$ .

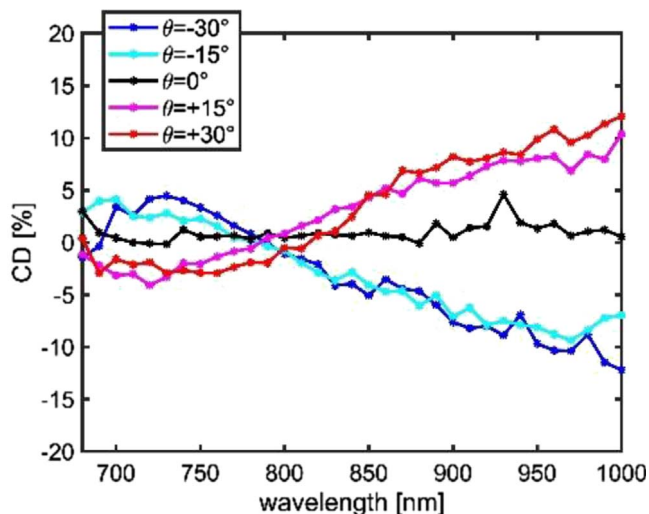


Fig. 3. CD dependence on the angle of incidence for the sample.

underscores the intricate nature of the sample's chirality under varying conditions of angle of incidence.

### 3 Conclusions

In conclusion, in this work, we have presented the CD behavior of metasurfaces made of polystyrene nanospheres asymmetrically coated with Ag. The metasurface was created by nanosphere lithography on soda-lime glass substrates and inclined evaporation of the metal. An extrinsic chiral response is detected as CD dependence on the angle of incidence of the input beam and the maximum CD is observed for a  $\theta$  angle of incidence equal to  $30^\circ$ .

Although photo-acoustic has been a widely used technique in the past, it is important to point out that its application was generally limited to the selection of a single color. However, through the use of current technique, we are now able to significantly extend the potential of photo-acoustic, allowing the analysis and selection of multiple wavelengths simultaneously.

#### Acknowledgments

A.B. acknowledges LASAFEM Sapienza Università di Roma Infrastructure Project No. MA31715C8215A268 and Sapienza Large Research Project 2022 No. RG1221816B6FA2E9. E.P.

acknowledges the RTDa-PON “ricerca e innovazione” 2014–2020 for financial and mobility support. We acknowledge M. Magi for technical support. T.C. acknowledges the financial support of the Physics and Astronomy Department through the project PRD-BIRD2022-Cesca. C. Skubisz acknowledges PNRR MUR project PE0000023-NQSTI.

#### Funding

This research received no external funding.

#### Conflicts of interest

The authors declare no conflict of interest.

#### Data availability statement

Data obtained in this work are not publicly available at this time but may be obtained from the authors upon reasonable request.

#### Author contribution statement

Conceptualization, E.P. and A.B.; methodology, E.P., G.L., A.B., and C. Sibilia; software, C. Skubisz and A.B.; fabrication, T.C, C. Scian and G. Mattei; measurements, E. P. and C. Skubisz; validation, A.B.; writing – original draft preparation, C. Skubisz; writing – review and editing, E.P. and A.B.

#### References

- 1 Kelvin L. (1894) *The molecular tactics of a crystal*, Clarendon Press, Oxford.
- 2 Hutt A.J., Tan S.C. (1996) Drug chirality and its clinical significance, *Drugs* **52**, 1–12.
- 3 Goerlitzer E.S.A., Puri A.S., Moses J.J., Poulikakos L.V., Vogel N. (2021) The beginner's guide to chiral plasmonics: mostly harmless theory and the design of large-area substrates, *Adv. Optical Mater.* **9**, 2100378.
- 4 Zhao Y., Askarpour A.N., Sun L., Shi J., Li X., Alù A. (2017) Chirality detection of enantiomers using twisted optical metamaterials, *Nat. Commun.* **8**, 14180.
- 5 Solomon M.L., Abendroth J.M., Poulikakos L.V., Hu J., Dionne J.A. (2020) Fluorescence-detected circular dichroism of a chiral molecular monolayer with dielectric metasurfaces, *J. Am. Chem. Soc.* **142**, 18304–18309.
- 6 Plum E., Liu X.-X., Fedotov V.A., Chen Y., Tsai D.P., Zheludev N.I. (2009) Metamaterials: optical activity without chirality, *Phys. Rev. Lett.* **102**, 113902.

- 7 De Leon I., Horton M.J., Schulz S.A., Upham J., Banzer P., Boyd R.W. (2015) Strong, spectrally-tunable chirality in diffractive metasurfaces, *Sci. Rep.* **5**, 13034.
- 8 Banzer P., Woźniak P., Mick U., De Leon I., Boyd R.W. (2016) Chiral optical response of planar and symmetric nanotrimers enabled by heteromaterial selection, *Nat Commun* **7**, 13117.
- 9 Zubritskaya I., Maccaferri N., Inchausti Ezeiza X., Vavassori P., Dmitrie A. (2018) Magnetic control of the chiroptical plasmonic surfaces, *Nano Lett.* **18**, 1, 302–307.
- 10 Petrucci G., Gabbani A., Faniayeu I., Pedrueza-Villalmanzo E., Cucinotta G., Atzori M., Dmitriev A., Pineider F. (21 June 2021.) Macroscopic magneto-chiroptical metasurfaces, *Appl. Phys. Lett.* **118**, 25, 251108.
- 11 Petronijevic E., Belardini A., Cesca T., Scian C., Mattei G., Sibilica C. (2021) Rich near-infrared chiral behavior in diffractive metasurfaces, *Phys. Rev. Applied* **16**, 014003.
- 12 Petronijevic E., Belardini A., Leahu G., Hakkarainen T., Piton M.R., Koivusalo E., Sibilica C. (2021) Broadband optical spin dependent reflection in self-assembled GaAs-based nanowires asymmetrically hybridized with Au, *Sci Rep.* **11**, 4316.
- 13 Spaeth P., Adhikari S., Le L., Jollans T., Pud S., Albrecht W., Bauer T., Caldarola M., Kuipers L., Orrit M. (2019) Circular dichroism measurement of single metal nanoparticles using photothermal imaging, *Nano Lett.* **19**, 12, 8934–8940.
- 14 Spaeth P., Adhikari S., Dieter Baaske M., Pud S., Ton J., Orrit M. (2021) Photothermal circular dichroism of single nanoparticles rejecting linear dichroism by dual modulation, *ACS Nano* **15**, 10, 16277–16285.
- 15 Leahu G., Petronijevic E., Li Voti R., Belardini A., Cesca T., Mattei G., Sibilica C. (2021) Diffracted beams from metasurfaces: high chiral detectivity by photothermal deflection technique, *Adv. Optical Mater.* **9**, 2100670.
- 16 Petronijevic E., Leahu G., Li Voti R., Belardini A., Scian C., Michieli N., Cesca T., Mattei G., Sibilica C. (2019) Photo-acoustic detection of chirality in metal-polystyrene metasurfaces, *Appl. Phys. Lett.* **114**, 053101.
- 17 Leahu G., Petronijevic E., Belardini A., Centini M., Sibilica C., Hakkarainen T., Koivusalo E., Rizzo Piton M., Suomalainen S., Guina M. (2017) Evidence of optical circular dichroism in GaAs-based nanowires partially covered with gold, *Adv. Opt. Mater.* **5**, 1601063.
- 18 Petronijevic E., Leahu G., Belardini A., Centini M., Li Voti R., Hakkarainen T., Koivusalo E., Guina M., Sibilica C. (2018) Resonant absorption in GaAs-based nanowires by means of photo-acoustic spectroscopy, *Int. J. Thermophys.* **39**, 45.
- 19 Belardini A., Centini M., Leahu G., Hooper D.C., Li Voti R., Fazio E., Haus J.W., Sarangan A., Valev V.K., Sibilica C. (2016) Chiral light intrinsically couples to extrinsic/pseudo-chiral metasurfaces made of tilted gold nanowires, *Sci. Rep.* **6**, 31796.
- 20 Najafabadi A.F., Pakizeh T. (2017) Analytical chiroptics of the 2D and 3D nanoantennas, *ACS Photonics* **4**, 6, 1447–1452.